



## The Holocene volcanism of Gran Canaria (Canary Islands, Spain)

A. Rodriguez-Gonzalez, F. J. Perez-Torrado, J. L. Fernandez-Turiel, M. Aulinas, R. Paris & C. Moreno-Medina

To cite this article: A. Rodriguez-Gonzalez, F. J. Perez-Torrado, J. L. Fernandez-Turiel, M. Aulinas, R. Paris & C. Moreno-Medina (2018) The Holocene volcanism of Gran Canaria (Canary Islands, Spain), Journal of Maps, 14:2, 620-629, DOI: [10.1080/17445647.2018.1526717](https://doi.org/10.1080/17445647.2018.1526717)

To link to this article: <https://doi.org/10.1080/17445647.2018.1526717>



© 2018 The Author(s). Published by Informa UK Limited, trading as Taylor & Francis Group on behalf of Journal of Maps



[View supplementary material](#)



Published online: 18 Oct 2018.



[Submit your article to this journal](#)



Article views: 680



[View Crossmark data](#)



## The Holocene volcanism of Gran Canaria (Canary Islands, Spain)

A. Rodriguez-Gonzalez <sup>a</sup>, F. J. Perez-Torrado <sup>a</sup>, J. L. Fernandez-Turiel <sup>b</sup>, M. Aulinas <sup>c</sup>, R. Paris <sup>d</sup> and C. Moreno-Medina <sup>e</sup>

<sup>a</sup>Instituto de Estudios Ambientales y Recursos Naturales (i-UNAT), Universidad de Las Palmas de Gran Canaria (ULPGC), Las Palmas de Gran Canaria, Spain; <sup>b</sup>Institute of Earth Sciences Jaume Almera, ICTJA-CISIC, Barcelona, Spain; <sup>c</sup>Departament de Mineralogia, Petrologia i Geologia Aplicada, Universitat de Barcelona (UB), Barcelona, Spain; <sup>d</sup>Laboratoire Magmas et Volcans, Université Clermont Auvergne, CNRS, IRD, OPGC, Clermont-Ferrand, France; <sup>e</sup>Departamento de Geografía, Grupo de Investigación Sociedades y Espacios Atlánticos (SEA), Universidad de Las Palmas de Gran Canaria (ULPGC), Las Palmas de Gran Canaria, Spain

### ABSTRACT

This work presents the first detailed map of the Holocene eruptions of Gran Canaria (Canary Islands, Spain). It provides complete and detailed information for all 24 Holocene eruptions of Gran Canaria, improving the knowledge of this recent volcanism and the assessment of volcanic hazards on the island. This map is a synthesis of collated and interpreted field data and topographic maps. We have integrated information obtained from: (1) detailed geological field surveys, (2) morphometric analysis of eruptive deposits, (3) high-resolution digital elevation models, and (4) aerial photographs.

### ARTICLE HISTORY

Received 28 July 2017  
Revised 12 September 2018  
Accepted 18 September 2018

### KEYWORDS

Holocene volcanism; Gran Canaria; Canary Islands; geological map

## 1. Introduction

The Canary Islands are one of the greatest natural laboratories for volcanology on our planet. This archipelago is volcanically active and all the islands, with the exception of La Gomera (Figure 1(b)), record the effects of Holocene volcanism. With the aim of improving the knowledge of monogenetic Holocene volcanism in the Canarian chain, we describe the age and areal distribution of Holocene volcanic products (cones, tephra air-fall deposits, and lava flows) of Gran Canaria, which is the third largest island by area and the most populated one of the Canarian Archipelago.

A comprehensive chronology of Holocene eruptions is essential for both the interpretation of the geological evolution and the assessment of volcanic hazards of a volcanic area. Here, the temporal succession of monogenetic volcanisms was inferred by geochronology, using radiocarbon dating of charcoal beneath and included in the lava flows, and relative dating based on the stratigraphic and geomorphologic relationships of the volcanic deposits.

The aims of this work are 1) to present a detailed cartography of the common units in monogenetic volcanic fields (cones, tephra air-fall deposits, and lava flows), together with geomorphologic and stratigraphic observations of these units, and with the surrounding substrate, and 2) to develop a methodology for generating palaeogeomorphological reconstructions of Digital Terrain Models (DTMs). Our reconstruction

considers two key evolutionary stages leading to the present day DTM (eruption affected by erosion), specifically pre-eruption (surface unaffected by eruptions) and immediate post-eruption (eruptive deposits unaffected by erosion) DTMs.

Comparison of these DTMs in a GIS framework gives 2D and 3D models that allow a proper understanding of the topographic changes that have taken place in the areas affected by Holocene volcanic eruptions in both the construction stages and their subsequent degradation.

## 2. Geological setting

### 2.1. Canary Islands

The Canary Islands are part of the group of archipelagos known as Macaronesia, in which Azores, Madeira and Cape Verde are also included. This region is located in the NE Atlantic Ocean between 14° and 40° N (subtropical environment), bordering the African coast (Figure 1(a)). The Canaries, which comprise seven main islands and several islets, are situated between 29° 25' and 27° 37' N and 18° 10' and 13° 20' W, and the total emerged area is 7490 km<sup>2</sup>. These islands developed in a geodynamic setting characterized by a thick, rigid and old (Jurassic) oceanic lithosphere lying close to a passive continental margin and on a slow-moving (2 cm/yr) plate (the African plate) (Silver, Russo, & Lithgow-Bertelloni, 1998).

**CONTACT** F. J. Perez-Torrado franciscojose.perez@ulpgc.es University Institute of Environmental Studies and Natural Resources (i-UNAT), Physics Department (Geology), Faculty of Marine Sciences, University of Las Palmas de Gran Canaria, University Campus of Tafira, Las Palmas de Gran Canaria 35017, Spain

© 2018 The Author(s). Published by Informa UK Limited, trading as Taylor & Francis Group on behalf of Journal of Maps

This is an Open Access article distributed under the terms of the Creative Commons Attribution License (<http://creativecommons.org/licenses/by/4.0/>), which permits unrestricted use, distribution, and reproduction in any medium, provided the original work is properly cited.

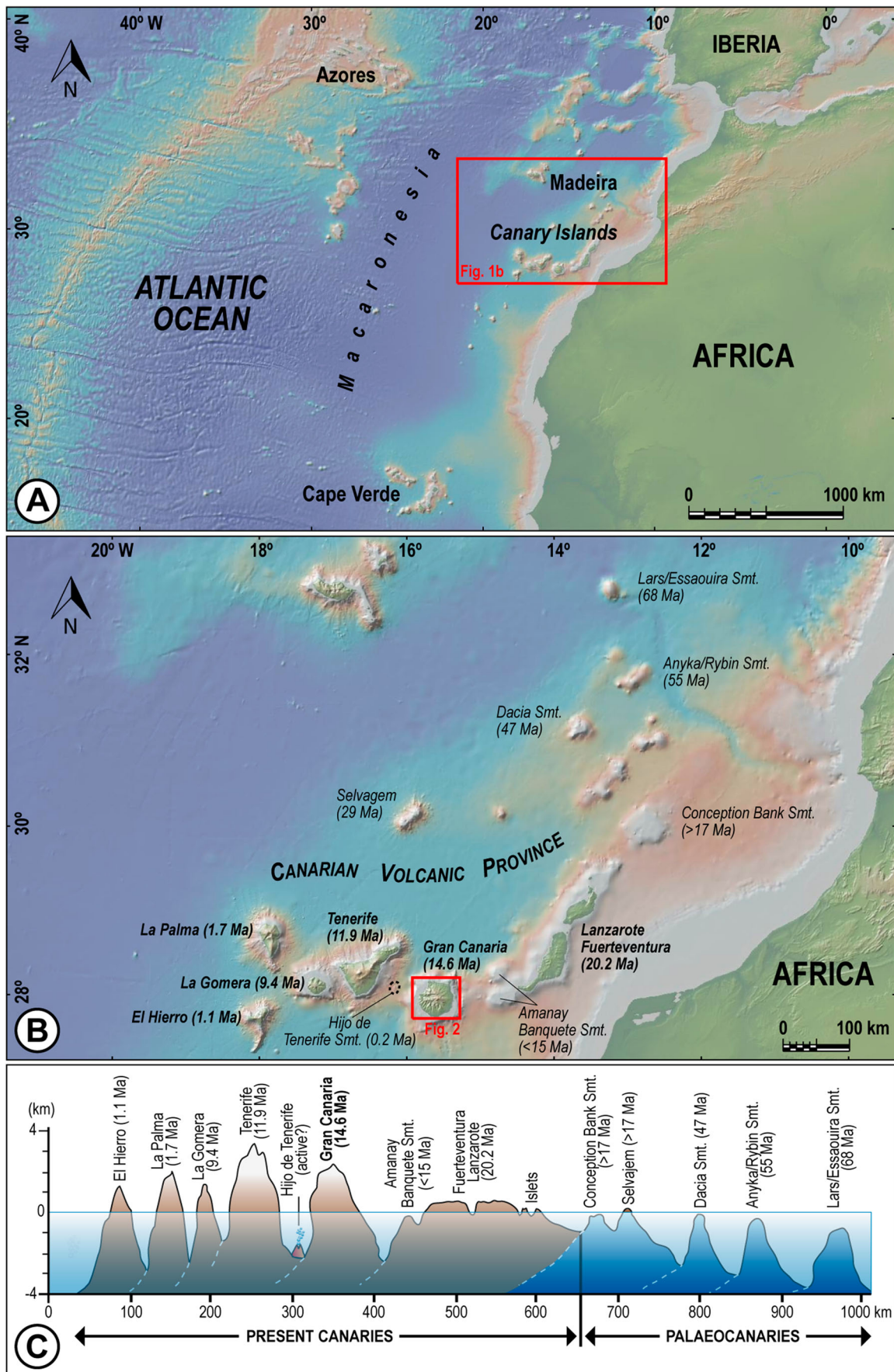


**Figure 1.** (a) Geographic setting of the Canary Islands in the group of islands of Macaronesia. (b) The Canary Volcanic Province, including the main islands and the associated seamounts. (c) Schematic diagram showing the chain of islands and seamounts that form the Canary Volcanic Province. The age increase toward the NE, from El Hierro (1.12 Ma) to Lars/Essaouira Seamount (68 Ma) (Geldmacher et al., 2001; Guillou et al., 2004; Zaczek et al., 2015).

The spatial and chronological evolution of the Canary Islands chain also comprises a group of seamounts located northeast of the archipelago (Figure 1(b)), with Lars/Essaouria, Anyka/Rybin, Dacia, Selvagem and Conception Bank being the largest ones. The archipelago and the seamounts, which form the Canary Volcanic Province, have an internal age-progression towards the SW, from the oldest age of circa 68 Ma for the Lars/Essaouria seamount to 1.12 Ma for the El Hierro island (Figure 1(b,c)) (Geldmacher, Hoernle, Bogaard, Duggen, & Werner, 2005; Geldmacher, Hoernle, van den Bogaard, Zankl, & Garbe-Schönberg, 2001; van den Bogaard, 2013; Zaczek et al., 2015). This progressive decrease in age, from east to west, is due to the movement of the African plate over a mantle plume (Carracedo et al., 1998, 2002; Holik, Rabinowitz, & Austin, 1991; Klügel, Hansteen, van den Bogaard, Strauss, & Hauff, 2011; Schmincke & Sumita, 2010; van den Bogaard, 2013). Similarly to other intraplate volcanic islands, the Canarian archipelago also displays the typical hotspot volcanic stages of evolution: juvenile (shield) stage, volcanic quiescence stage and rejuvenated stage. While the more western islands (El Hierro and La Palma) are still in the juvenile stage, characterized by high eruption rates and fast volcanic growth of the islands, the eastern islands (Fuerteventura and Lanzarote) are in a terminal rejuvenated stage, with a predominance of erosive processes on the volcanic deposits (Carracedo et al., 1998, 2002).

## 2.2. Gran Canaria

Gran Canaria, a nearly circular island, is located at the centre of the Canarian archipelago. It is the third largest island by surface area (1532 km<sup>2</sup>), with a diameter of 45 km and a maximum elevation of 1950 m above sea level (a.s.l.) at the centre of the island (Pico de las Nieves). This configuration led to the formation of a set of dense radial networks of deep ravines (known as *barrancos* in the local toponomy) that dissect the island, forming a rugged topography with a mean slope value of 21.7°. The main geomorphologic and structural features of Gran Canaria, which are related to the volcanic evolution of the island, divide the island into two equal parts following a NW–SE line that coincides with a Pliocene rift zone. The older, SW part, known as Palaeocanaria, is predominately formed of Miocene volcanic products. In contrast, the younger, NE portion of the island, known as Neocanaria, concentrates the Plio-Quaternary volcanism (Boucart & Jérémie, 1937; Carracedo et al., 2002; Guillou, Torrado, Machin, Carracedo, & Gimeno, 2004). Additionally, Gran Canaria features a marked climatic zonation with arid to semiarid conditions on the southern flanks and humid to sub-humid conditions on the northern flanks. Overall, the subaerial growth of Gran Canaria comprises the two main phases of construction of an

intraplate oceanic island (shield and post-erosive stages), which are both superbly represented in the island (Figure 2(a)).

The oldest evolutionary volcanic stage recorded sub-aerially in Gran Canaria (ca. 14.5–7.3 Ma) was characterized by the development of a basaltic shield volcano and related gravitational landslides (Figure 2(b)). It was followed by a vertical caldera collapse (Caldera de Tejeda) with an enormous volume of associated ignimbrites (Figure 2(c)) and a post-caldera resurgence with syenitic cone-sheet intrusions (Figure 2(d)). The volcanic period of quiescence (ca. 8.8–5.5 Ma) included the deposition of the most prominent sedimentary deposits of the island (Las Palmas Detritic Formation). Finally, a rejuvenated stage (ca. 5.5 Ma to present) generated the Roque Nublo stratovolcano (Figure 2(e)) and the Post-Roque Nublo volcanism with a rift zone aligned NW–SE (Figure 2(f)) (Aulinas et al., 2010a, 2010b; Carracedo et al., 2002; Guillou et al., 2004; Hansen, 2009; Perez-Torrado, Carracedo, & Mangas, 1995).

## 2.3. The Holocene volcanism

All Holocene (Post-Roque Nublo) volcanism of Gran Canaria is geographically restricted to the northern half of the island, in both the western and the eastern volcanic areas (Figure 2(a)). The most distinctive geomorphologic characteristic of these eruptions is the emplacement of lava flows at the bottom of *barrancos*; the latter were formed during the most recent incision phase (Figure 3(a)). A total of 24 Holocene eruptions were identified on the island (Rodriguez-Gonzalez, 2009; Rodriguez-Gonzalez et al., 2009, 2011, 2012). The erosional history of Holocene volcanic edifices is in the early stages of degradation (Davidson & De Silva, 2000; Rodriguez-Gonzalez, 2009; Rodriguez-Gonzalez et al., 2011), with a geomorphic signature characterized by a fresh, young cone with a sharp profile (Figure 3(b)) and pristine lava flow (Figure 3(c)). The erosion affected the volcanic materials erupted during Holocene times and their substratum dissimilarly. Lava flows (the most resistant material) are very well preserved, while pyroclastic deposits have experienced considerable erosion (Figure 3(d)).

## 3. Methods and materials

The existing geological maps of Gran Canaria consist of the 1:100,000 map (Balcells, Barrera, & Gómez, 1992) and fifteen 1:25,000 maps published by the Spanish Geological Survey (IGME). The 1:25,000 maps covering the Holocene volcanic units are 1109-I (Santa Brígida); 1109-II (Telde) and 1101-III-IV (Aruca) (Balcells & Barrera, 1990a, 1990b, 1990c); 1109-IV (Teror) and 1100-I-II (Agaete) (Balcells, Barrera, & Gómez, 1990a, 1990b); and 1108-I (Vecindad de Enfrente) and 1109-III (San Bartolomé de Tirajana)

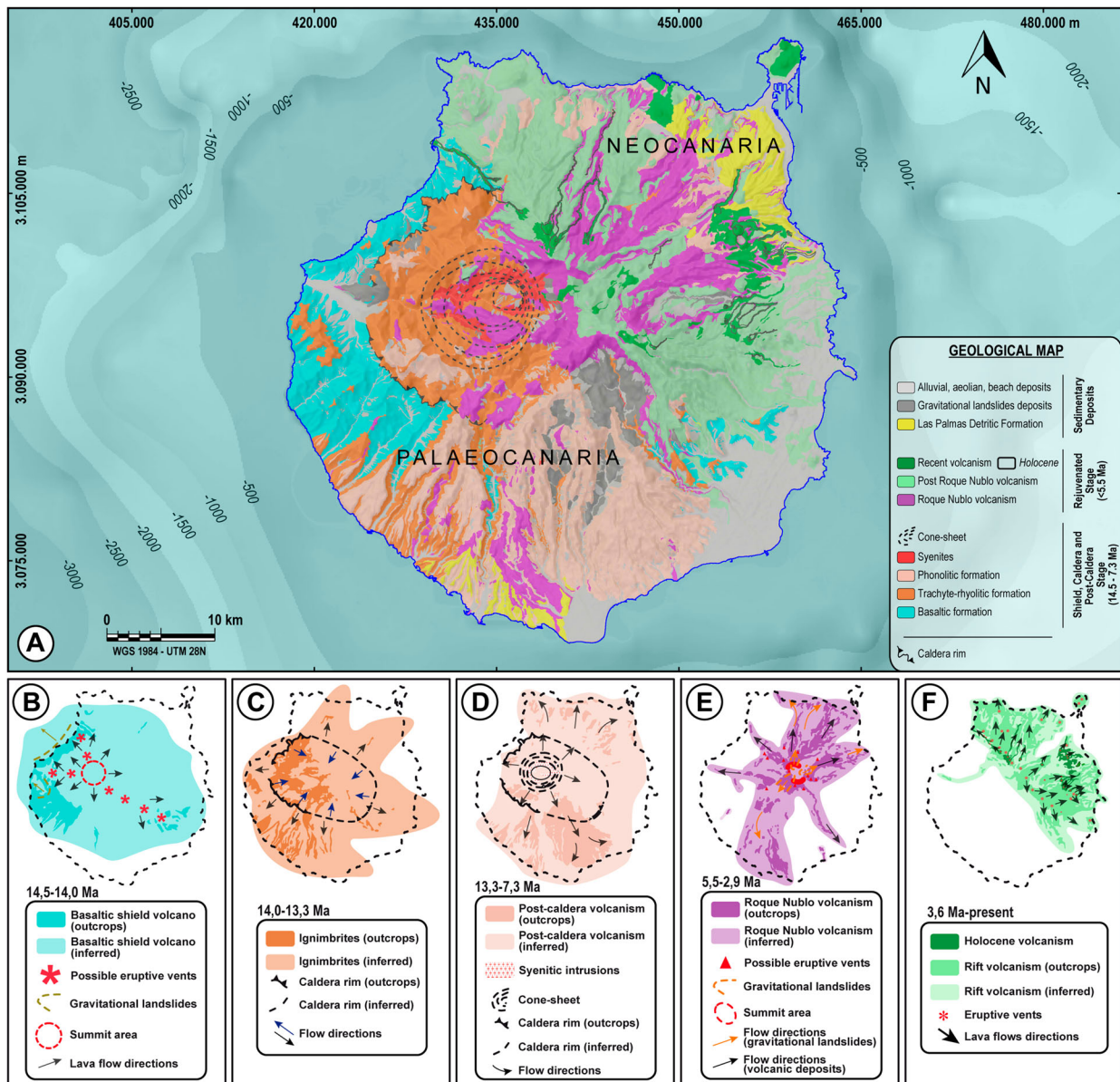


**Figure 2.** (a) Geological map of Gran Canaria (modified from Barrera & García Moral, 2011) with bathymetry data derived from Global Multi-Resolution Topography (GMRT) in GeoMap (Ryan et al., 2009). (b) Distribution of volcanic products corresponding to the initial stage of the shield building, marking both the possible rift alignments and the landslides that occurred at this stage. (c) Distribution of trachytic-rhyolitic deposits emitted in the first phase of caldera resurgence and delimitation of the Caldera de Tejeda. (d) Distribution of trachytic-phonolitic materials in the intra- and extra-calderic domains and intrusive magmatism. (e) After the volcanic quiescence stage, volcanic activity was reactivated with the formation of the stratovolcano Roque Nublo. (f) Distribution of Post-Roque Nublo volcanism, linked firstly with a rift type NW–SE structure and later with dispersion of temporal space (b, c, d, e and f modified from Rodríguez-Gonzalez, 2009).

(Barrera & Gómez, 1990a, 1990b). Later on, the Spanish Geological Survey (IGME) systematized the 1:25,000 geological maps in digital format (IGME, 2008).

Detailed field work confirmed that the 1: 25,000 scale geological maps are not sufficiently detailed for the characterization of the Holocene volcanism in order to carry out a precise quantification of important morphometric parameters such as volumes, surfaces and lengths. Furthermore, we identified some uncertainties in the assignation of lava flows to volcanic vents, the delimitation of the lava flow contacts, and the eruption ages in both the printed and digital

versions of these previous 1:25,000 scale geological maps. As a consequence, existing IGME maps provided only preliminary guidance, and we produced new 1:5,000 scale maps for each Holocene eruption observed in the field (Rodríguez-Gonzalez, 2009).

In this way, the field work consisted of reproducing the observations on a geological map with the appropriate symbology by representing the existing stratigraphic units and related geological structures. We carried out an extensive field campaign focused on the collection of information on the Holocene eruptions, including their geographical position and contact with older units, in many cases obtained by a handheld global

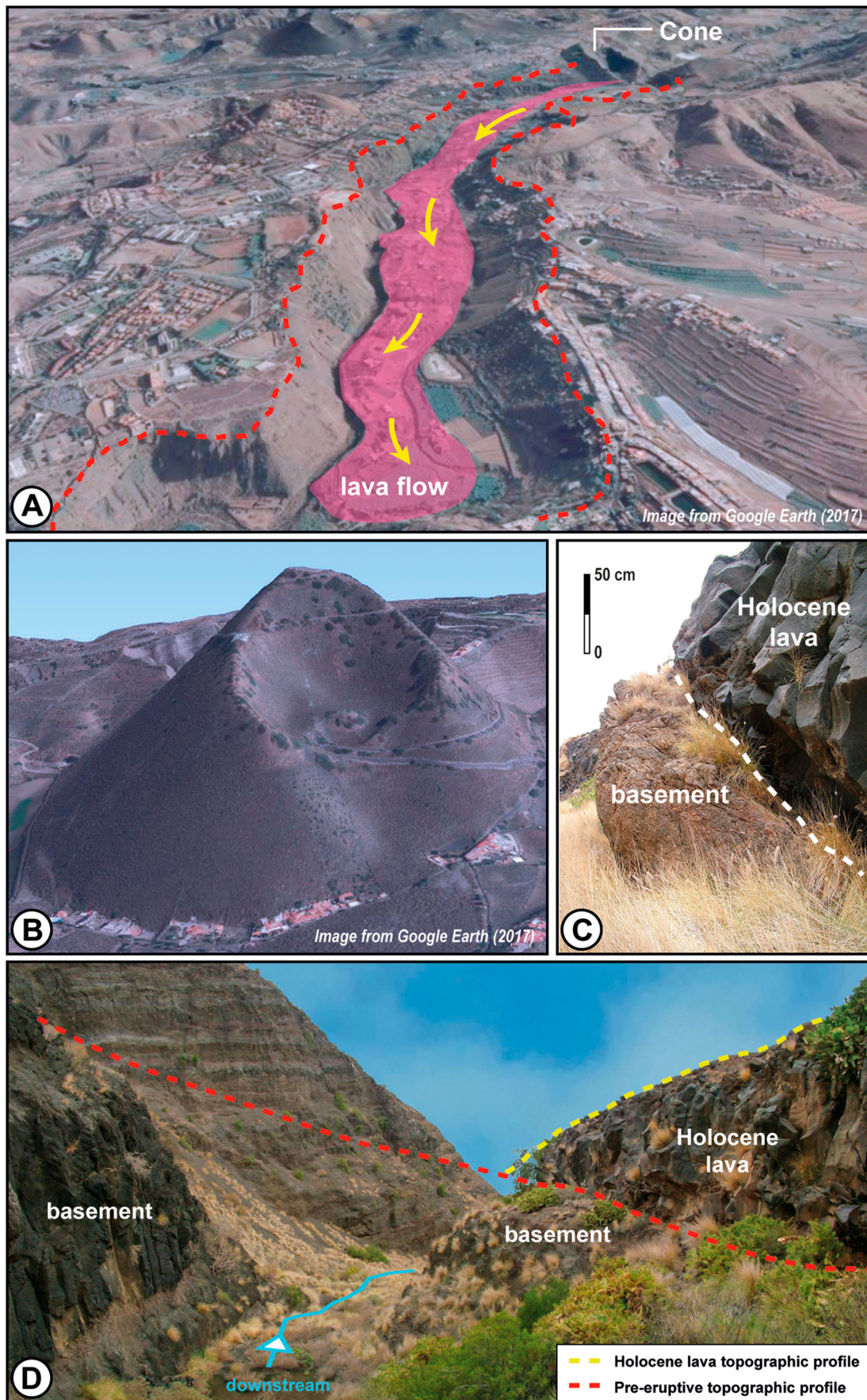


**Figure 3.** (a) Landscape perspective of a Holocene eruption (El Lentiscal) showing the emission centre and lava flow at the bottom of a *barranco*. (b) Cone with horseshoe open crater (Pico Bandama). (c) Contact of the Holocene lava flow (Fagajesto) with the basement. (d) General view of the erosive effects of the *barranco* on the basement and Holocene lava flow, and reconstructions of the different palaeotopographic profiles.

positioning system (GPS) receiver. We worked in the field mainly using digital topographic maps (1:5,000) and high-resolution coloured aerial photographs (1:18,000) from GRAFCAN (Public Company of Cartography of the Canary Islands) ([www.grafcan.es](http://www.grafcan.es)) and the LIDAR DEM (reclassified to 5 m resolution) from the National Geographic Institute (IGN) (available at: <http://centrodedescargas.cnig.es/CentroDescargas/index.jsp>).

A spatial database was designed and implemented with different data sets and layers containing all information obtained for this study. These data sets comprise volcanic vents, eruptive fissures, and all those observations related to geomorphology and morphometry, geochemistry, and petrology as well as  $^{14}\text{C}$  ages (Aulinas et al., 2010a, 2010b; Kissel et al., 2015a, 2015b; Rodriguez-Gonzalez, 2009; Rodriguez-Gonzalez, Fernandez-Turiel, Perez-Torrado, Gimeno, & Aulinas, 2010; Rodriguez-Gonzalez et al., 2009, 2011, 2012). All these elements were mapped using the WGS84 UTM 28N coordinate system.

The method of generating the palaeogeomorphological reconstruction is described in Rodriguez-

Gonzalez et al. (2010, 2012). In summary, to reconstruct the pre-eruption surface, we generate multiple detailed geological cross-sections of each lava flow and volcanic cone. To do this, we use the present day 1:5,000 scale geological maps for the 24 Holocene eruptions of Gran Canaria, which distinguish between different volcanic units (i.e. volcanic cone, lava flow and tephra air-fall), and consider all field morphometric data (e.g. lava flow thickness variations along its lengths, height variations between the volcanic units' contacts and the bottom of *barrancos*, etc.). All this information was used to modify the present-day contour topographic maps at 1:5,000 scale of GRAFCAN (see Figures 5 and 6 of Rodriguez-Gonzalez et al., 2010). The results are three DTMs corresponding to the pre-, post-, and present day eruption surfaces (Rodriguez-Gonzalez, 2009; Rodriguez-Gonzalez et al., 2010, 2011, 2012). Two-dimensional morphometric parameters (i.e. volcanic cone area, crater rim axis, lava flow area, lava flow length, sinuosity, and width of pre-eruption *barranco*, etc.) are obtained from each DTM by applying appropriate GIS tools.

**Table 1.** Radiocarbon, calibration ages and stratigraphic relationships, with IntCal13 atmospheric curve (Reimer et al., 2013), of Holocene eruptions of Gran Canaria. Data from Rodriguez-Gonzalez et al. (2009). Radiocarbon age error reported as  $2\sigma$ .

N°	Eruption name	Method <sup>a</sup>	Laboratory <sup>b</sup>	$\delta^{13}\text{C}$ (o/oo)	Conventional radiocarbon age	Calibrated age
					(a BP) and/or stratigraphic relationship	(cal a BP and % probability) Version OxCal 4.2 [104], Curve IntCal13
1	Pico Bandama	AMS	1	–	1970 ± 70 Above n° 2	2110–1770 (93.4%)
2	Caldera Bandama	–	–	–	Beneath n° 1 Above n° 9	–
3	El Garañón	AMS	2	–24.1	1990 ± 40	2040–1860 (94.5%)
4	Doramas	AMS	2	–25.0	2420 ± 40	2540–2350 (69.2%)
5	El Lentiscal	AMS	1	–	2450 ± 60 Beneath n° 1	2720–2360 (95.4%)
6	Montaña de El Gallego	–	–	–	Above n° 9	–
7	Cuesta de Las Gallinas	–	–	–	Above n° 9	–
8	Montaña Rajada	–	–	–	Above n° 9	–
9	Sima de Jinámar	CRT	2	–23.9	2470 ± 50 Beneath n° 2, 6, 7 and 8 Above n° 12	2720–2360 (95.4%)
10	Montaña Negra de Jinámar	CRT	2	–19.8	2540 ± 60 Beneath n° 7 Above n° 12	2760–2430 (94.6%)
11	Montaña Pelada II	–	–	–	Beneath n° 2 Above n° 12	–
12	Montaña Pelada	–	–	–	Beneath n° 9, 10 and 11	–
13	Berrazales	–	–	–	Above n° 17	–
14	Jabalobos	CRT	2	–22.8	2760 ± 60 Above n° 17	3000–2750 (95.4%)
15	Pinos de Gáldar	AMS	1	–	2830 ± 60 Above n° 16	3080–2790 (92.3%)
16	Montañón Negro	AMS	1	–	2970 ± 70 Beneath n° 15 Above n° 18	3350–2950 (95.4%)
17	Fagajesto	AMS	2	–27.8	3030 ± 90 Beneath n° 13 and 14	3400–2960 (94.4%)
18	Caldereta Valleseco	–	–	–	Beneath n° 16	–
19	San Mateo	AMS	1	–	5790 ± 70	6744–6430 (95.1%)
20	Montaña de Santidad	–	–	–	Beneath n° 2 Above n° 21 and 23	–
21	El Melosal	–	–	–	Beneath n° 2 and 20	–
22	El Hoyo	AMS	1	–	5830 ± 100 Beneath n° 2	6880–6410 (95.4%)
23	Montaña de Barros II	–	–	–	Beneath n° 20	–
24	El Draguillo	CRT	2	–22.6	10610 ± 190	12910–11950 (94.9%)

<sup>a</sup>AMS, accelerator mass spectrometry; CRT, conventional radiometric technique.

<sup>b</sup>1, Laboratoire des Sciences du Climat et de l'Environnement, Gif sur Yvette (France); 2, Beta Analytic Inc., Florida (USA).

On the other hand, 3D morphometric parameters (i.e. volumes of volcanic cone and lava flow, volumes of eroded substratum, height of volcanic cone, etc.) are obtained from the GIS cut-and-fill process between the DTMs. A DTM resolution of  $5 \times 5$  m pixel size is appropriate for the accurate quantification of all the morphometric parameters of interest (Rodríguez-González et al., 2010).

#### 4. Chrono-stratigraphic and volcano-structural analyses

##### 4.1. Chrono-stratigraphic correlations

The available conventional radiocarbon and calibrated Holocene ages are shown in Table 1. Thirteen charcoal samples were obtained from eruptions that had been reliably fixed stratigraphically among other older volcanic materials or undated Holocene eruptions (Rodríguez-González et al., 2009).

The temporal distribution of the conventional radiocarbon ages allows eruptions to be grouped into

three periods of volcanic activity (Rodríguez-González et al., 2009). The oldest period consists of one eruption, El Draguillo, dated at  $10,610 \pm 190$  yr BP, and its deposits are, unsurprisingly, the most affected by erosion. The second period (5 eruptions) spans 5700–6000 yr BP. The most recent period (18 of the 24 eruptions) spans 1900–3200 yr BP. The length of volcanic quiescence is variable, decreasing towards the present.

##### 4.2. Volcano-structural analyses

Field studies by Rodríguez-González et al. (2009, 2012) showed that these Holocene eruptions typically constructed Strombolian cones (up to 215 m in height) and erupted relatively long lava flows (up to 10 km). The total volume of these eruptions is  $\sim 0.4$  km<sup>3</sup> (46% as tephra fall, 42% as cinder cone deposits and 12% as lava flows). The relatively low eruption rate (0.04 km<sup>3</sup>/ka) during the past 11 ka, in the late stage of evolution of Gran Canaria, is consistent with the volcano-tectonic framework of the Canary Islands (Carracedo et al., 2002; Rodríguez-González et al., 2009).

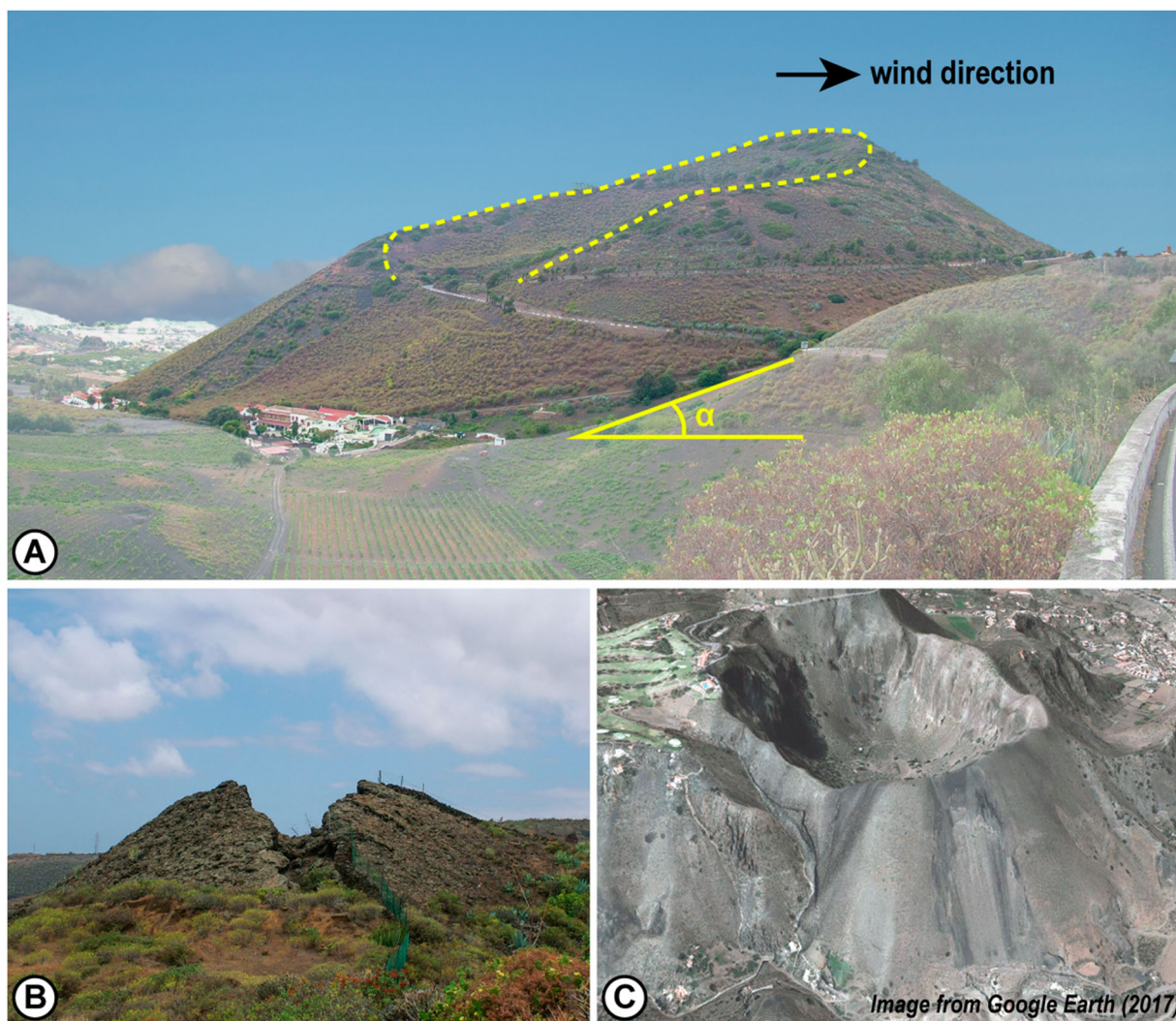


**Figure 4.** (a) Strombolian cone (Pico Bandama) showing the opening of the horseshoe crater (dotted yellow line) and the middle angle of the slope where the cone emerges; the direction of prevailing winds during the eruption are marked. (b) Vent related to a hornito (Montaña Rajada). (c) Aerial perspective of the phreatomagmatic Caldera of Bandama.

#### 4.2.1. Vents

The Gran Canaria Holocene volcanic cones are mainly typical scoria cones resulting from Strombolian-type eruptions, according to the classification of the scoria cones (Martin & Németh, 2006; Rodriguez-Gonzalez et al., 2011). Only six scoria cones display evidence of considerable influence by hydromagmatic eruptive processes.

This volcanism mainly produced small monogenetic Strombolian cones (~70 m in height and ~400 m in basal diameter). They usually have a horseshoe-shaped opening which is conditioned by the original relief and wind prevalence (Figure 4(a)). Occasionally, lava flows were emitted directly from hornitos and small fissures (Figure 4(b)). The presence of some volcanic products cropping out tens of kilometres away from maars is also noteworthy (Figure 4(c)) (Rodriguez-Gonzalez et al., 2012).

Strombolian eruptions present a mantle of tephra air-fall deposits consisting mainly of lapilli, although

volcanic bombs are also common in the deposits closest to the eruption vent. These tephra air-fall deposits extend in the direction of the prevailing winds, which in the case of the Canary Islands are the trade winds that blow relatively steadily from the NE and NW directions.

#### 4.2.2. Lava flows

As explained in the ‘Methods and Materials’ section, field work illuminated some uncertainties reported on previous IGME 1:25,000 scale geological maps related to the delimitation of lava flow contacts and in the assignation of some flows to the corresponding vents. The more detailed cartography presented in this work resolves these inconsistencies and allows a better understanding of the rheological properties of the Holocene lava flows.

Depending on the volume and emission rate of magma, the Holocene basaltic lava flows of Gran Canaria can cover large areas and reach the coast,

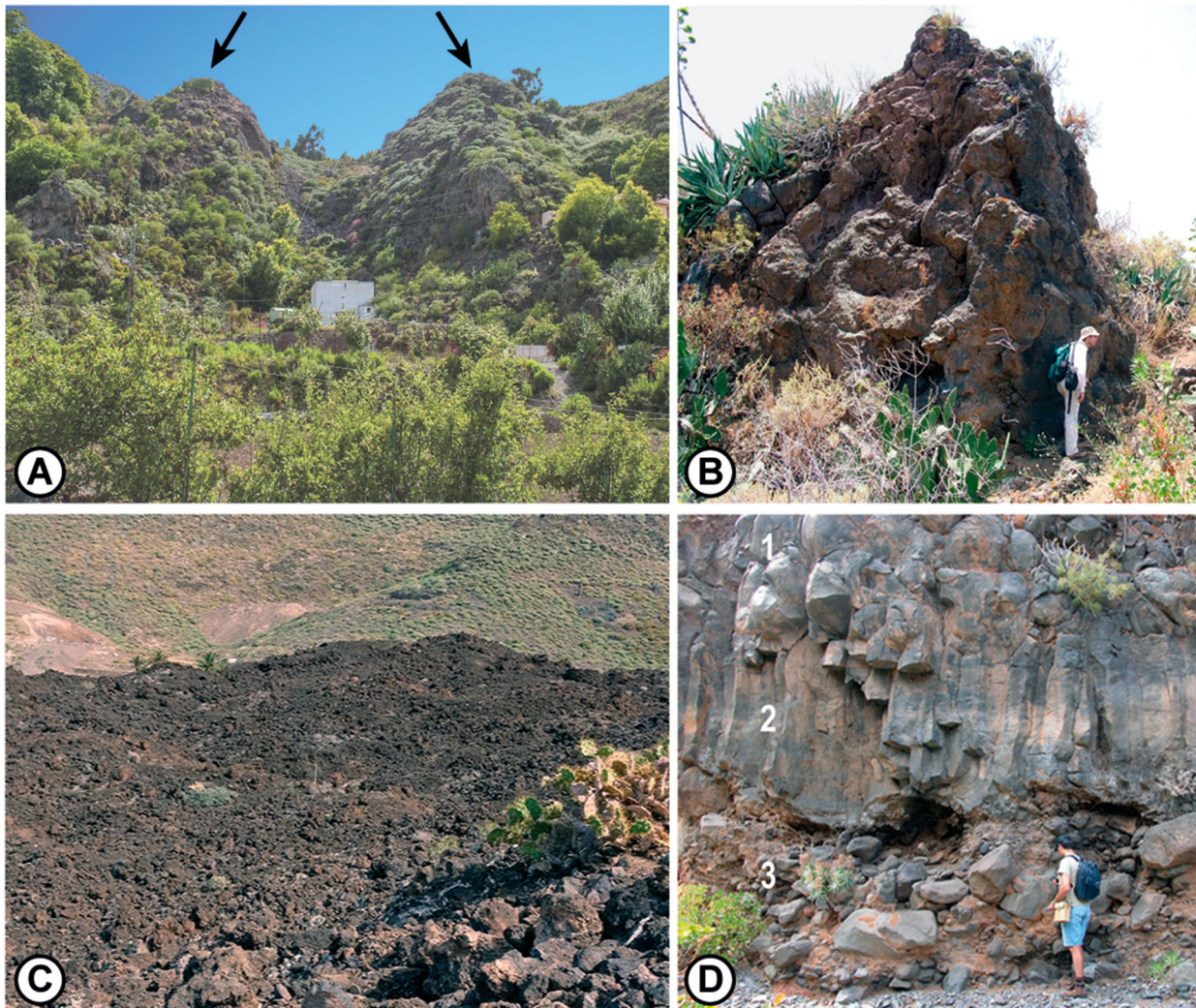


**Figure 5.** (a) General view of a lava channel indicating (black arrows) the levees. (b) Example of erratic block on the lava flow of the El Hoyo eruption. (c) Lava flow from Fagajesto eruption, with well-preserved a'a type morphologies (*malpais*), and a large number of small mounds built by scoria. (d) Lava flow from El Draguillo eruption, elevated from the current *barranco* due to erosion. Different morphologies are present in the same lava flow: ball form (1) and columnar form (2). The substrate is formed by conglomerate alluvial sediments (3).

with lengths from 100 m to 10 km. The smallest eruptive centres have shorter lava flows and are too small in volume to fill in *barrancos*. The length, thickness, and area occupied by lava flows depend on the morphology of the terrain and the presence or absence of obstacles (Rodríguez-González et al., 2012). Among all the studied lavas, the only lava flow which reached the coast and formed a platform is from the Fagajesto, in the west of Gran Canaria. Lava flow morphology is independent of lava flow length. Many lava flows form channels or tubes, and levees formed for numerous flow events are common (Figure 5a). Additionally, there are many erratic blocks on the surfaces of lava flows (Figure 5b). The average thickness of the lava flows varies from 1 to 20 m, with medium widths ranging from 50 to 400 m (Rodríguez-González et al., 2012). Most of these lava flows, which are mainly of a'a type (*malpaís* in the local toponymy, Figure 5(c)), commonly show columnar and spheroidal disjunctions (Figure 5(d)).

## 5. Conclusions

The first detailed map of the 24 Holocene eruptions of Gran Canaria is presented here and integrates all volcanic forms including vents, lava flows, tephra air-fall deposits, and levees, among others. The map is produced in DIN A1 format. It integrates several maps of the twenty-four Holocene eruptions at different scales, from 1:55,000 to 1:7,000. This map is accompanied by an example of a cross-section showing the reconstructed palaeosurface affected by the Lentiscal eruption (cone) and a simplified geological map of Gran Canaria with the location of the Holocene maps.

This contribution consolidates and highlights knowledge of the Holocene volcanism of Gran Canaria, providing an upgraded cartographic document in which all mapped volcanic elements are spatially and temporally consistent with each other. This information is especially of interest for the assessment of volcanic hazard in Gran Canaria, because the past is the key to the future in the forecasting of new eruptions.

## Software

Georeferencing and digitization of the Holocene eruptions were originally performed using TNTmips 6.9 but for this work we used TNTmips 2015, ESRI ArcGIS 10.5 and QGIS 2.18.4. The 3D images on the map were produced using the ArcScene module and Qgis2-threejs plugin in QGIS 2.18.4. The topographic profiles were produced using the profile tool for TNTmips 2015, the GeoMap application for bathymetric maps, and Microsoft Excel 2016. The final design was carried out using Adobe Illustrator CC.

## Geolocation information

Gran Canaria Island, Canary Islands, Spain. Please download this Google Earth file: <https://www.dropbox.com/s/geg9oeet1r2kfhv/Geolocation%20Information.kmz?dl=0>

## Acknowledgements

The research carried out to develop this map, including field work, radiometric dating, geomorphology, petrology and geochemistry, was funded by the Spanish Ministry of Education and Science through the project CGL2004-04039BTE and the Canarian Government through the projects PB96-0243 and PI2002/148. We especially acknowledge Dr. G. Beconyité, Dr. J.C. Carracedo, and Dr. N.I. Deligne for their critical reading and useful suggestions on the manuscript and map.

## Disclosure statement

No potential conflict of interest was reported by the authors.

## Funding

The research carried out to develop this map, including field work, radiometric dating, geomorphology, petrology and geochemistry, was funded by the Spanish Ministry of Education and Science for the research project CGL2004-04039/BTE and the Canarian Government for the research project PI2002/148; Instituto de Estudios Ambientales y Recursos naturales (i-UNAT), ULPGC.

## ORCID

A. Rodríguez-González  <http://orcid.org/0000-0003-0688-0531>

F.J. Pérez-Torrado  <http://orcid.org/0000-0002-4644-0875>

J.L. Fernández-Turiel  <http://orcid.org/0000-0002-4383-799X>

M. Aulinas  <http://orcid.org/0000-0003-3795-3537>

R. Paris  <http://orcid.org/0000-0003-4569-5187>

C. Moreno-Medina  <http://orcid.org/0000-0002-3067-5696>

## References

- Aulinas, M., Gimeno, D., Fernández Turiel, J. L., Font, L., Pérez-Torrado, F. J., Rodríguez-González, A., & Nowell, G. M. (2010a). Small-scale mantle heterogeneity on the source of the Gran Canaria (Canary Islands) Pliocene-Quaternary magmas. *Lithos*, 119(3-4), 377–392. doi:10.1016/j.lithos.2010.07.016
- Aulinas, M., Gimeno, D., Fernández Turiel, J. L., Pérez-Torrado, F. J., Rodríguez-González, A., & Gasperini, D. (2010b). The Plio-Quaternary magmatic feeding system beneath Gran Canaria (Canary Islands, Spain): constraints from thermobarometric studies. *Journal of the Geological Society*, 167(4), 785–801. doi:10.1144/0016-76492009-184
- Balcells, R., & Barrera, J. L. (Cartographer). (1990a). Geological Map 1109-I Santa Brígida.
- Balcells, R., & Barrera, J. L. (Cartographer). (1990b). Geological Map 1109-II Telde.
- Balcells, R., & Barrera, J. L. (Cartographer). (1990c). Geological Map 1101-II-IV Arucas.
- Balcells, R., Barrera, J. L., & Gómez, J. A. (Cartographer). (1990a). Geological Map 1109-IV Teror.

- Balcells, R., Barrera, J. L., & Gómez, J. A. (Cartographer). (1990b). Geological Map 1100-I-II Agaete.
- Balcells, R., Barrera, J. L., & Gómez, J. A. (Cartographer). (1992). Geological Map 21-21/21-22 Isla de Gran Canaria.
- Barrera, J. L., & García Moral, R. (Cartographer). (2011). Mapa Geológico de Canarias.
- Barrera, J. L., & Gómez, J. A. (Cartographer). (1990a). Geological Map 1108-I Vecindad de Enfrente.
- Barrera, J. L., & Gómez, J. A. (Cartographer). (1990b). Geological Map 1109-III San Bartolomé de Tirajana.
- Boucart, J., & Jérémine, E. (1937). La Grande Canarie. *Bulletin Volcanologique*, 2(1), 3–77. doi:10.1007/bf03028397
- Carracedo, J. C., Day, S., Guillou, H., Rodriguez-Badiola, E. R., Canas, J. A., & Perez-Torrado, F. J. (1998). Hotspot volcanism close to a passive continental margin: The Canary Islands. *Geological Magazine*, 135(5), 591–604. doi:10.1017/s0016756898001447
- Carracedo, J. C., Perez-Torrado, F. J., Ancochea, E., Meco, J., Hernán, F., Cubas, C. R., ... Ahijado, A. (2002). Cenozoic volcanism: II the Canary Islands. In F. A. W. Gibbons, & T. Moreno (Eds.), *The geology of Spain* (pp. 438–472). Londres: Geological Society of London.
- Davidson, J., & De Silva, S. (2000). *Composite volcanoes*. San Diego: Academic Press.
- Geldmacher, J., Hoernle, K., Bogaard, P. V. D., Duggen, S., & Werner, R. (2005). New <sup>40</sup>Ar / <sup>39</sup>Ar age and geochemical data from seamounts in the Canary and Madeira volcanic provinces: Support for the mantle plume hypothesis. *Earth and Planetary Science Letters*, 237(1–2), 85–101. doi:10.1016/j.epsl.2005.04.037
- Geldmacher, J., Hoernle, K., van den Bogaard, P., Zankl, G., & Garbe-Schönberg, D. (2001). Earlier history of the ≥70-Ma-old Canary hotspot based on the temporal and geochemical evolution of the Selvagen Archipelago and neighboring seamounts in the eastern North Atlantic. *Journal of Volcanology and Geothermal Research*, 111(1–4), 55–87. doi:10.1016/S0377-0273(01)00220-7
- Guillou, H., Torrado, F. J. P., Machin, A. R. H., Carracedo, J. C., & Gimeno, D. (2004). The Plio-Quaternary volcanic evolution of Gran Canaria based on new K-Ar ages and magneto stratigraphy. *Journal of Volcanology and Geothermal Research*, 135(3), 221–246.
- Hansen, A. (2009). *Volcanología y geomorfología de la etapa de rejuvenecimiento plio-pleistocena de Gran Canaria (Islas Canarias)*. Las Palmas de Gran Canaria: University of Las Palmas de Gran Canaria.
- Holik, J. S., Rabinowitz, P. D., & Austin, J. A. (1991). Effects of Canary hotspot volcanism on structure of oceanic crust off Morocco. *Journal of Geophysical Research: Solid Earth*, 96(B7), 12039–12067. doi:10.1029/91JB00709
- IGME. (2008). *Plan geode de cartografía geológica continua*. Instituto Geológico y Minero de España. Cartografía digital. Retrieved from <http://cuarzo.igme.es/sigeco/>
- Kissel, C., Laj, C., Rodriguez-Gonzalez, A., Perez-Torrado, F., Carracedo, J. C., & Wandres, C. (2015a). Holocene geomagnetic field intensity variations: Contribution from the low latitude Canary Islands site. *Earth and Planetary Science Letters*, 430, 178–190. doi:10.1016/j.epsl.2015.08.005
- Kissel, C., Rodriguez-Gonzalez, A., Laj, C., Perez-Torrado, F., Carracedo, J. C., Wandres, C., & Guillou, H. (2015b). Paleosecular variation of the earth magnetic field at the Canary Islands over the last 15 ka. *Earth and Planetary Science Letters*, 412, 52–60. doi:10.1016/j.epsl.2014.12.031
- Klügel, A., Hansteen, T. H., van den Bogaard, P., Strauss, H., & Hauff, F. (2011). Holocene fluid venting at an extinct Cretaceous seamount, Canary archipelago. *Geology*, 39(9), 855–858. doi:10.1130/g32006.1
- Martin, U., & Németh, K. (2006). How Strombolian is a “Strombolian” scoria cone? Some irregularities in scoria cone architecture from the Transmexican Volcanic Belt, near Volcán Ceboruco, (Mexico) and Al Haruj (Libya). *Journal of Volcanology and Geothermal Research*, 155(1–2), 104–118. doi:10.1016/j.jvolgeores.2006.02.012
- Perez-Torrado, F. J., Carracedo, J. C., & Mangas, J. (1995). Geochronology and Stratigraphy of the Roque Nublo Cycle, Gran Canaria, Canary Islands. *Journal of the Geological Society*, 152, 807–818.
- Reimer, P. J., Bard, E., Bayliss, A., Beck, J. W., Blackwell, P. G., Ramsey, C. B., ... van der Plicht, J. (2013). Intcal13 and Marine13 Radiocarbon Age Calibration Curves 0–50,000 Years cal BP. *Radiocarbon*, 55(4), 1869–1887. doi:10.2458/azu\_js\_rc.55.16947
- Rodriguez-Gonzalez, A. (2009). *El vulcanismo holoceno de Gran Canaria: Aplicación de un sistema de información geográfico*. Las Palmas de Gran Canaria: University of Las Palmas de Gran Canaria.
- Rodriguez-Gonzalez, A., Fernandez-Turiel, J. L., Perez-Torrado, F. J., Aulinas, M., Carracedo, J. C., Gimeno, D., ... Paris, R. (2011). GIS methods applied to the degradation of monogenetic volcanic fields: A case study of the Holocene volcanism of Gran Canaria (Canary Islands, Spain). *Geomorphology*, 134(3–4), 249–259. doi:10.1016/j.geomorph.2011.06.033
- Rodriguez-Gonzalez, A., Fernandez-Turiel, J. L., Perez-Torrado, F. J., Gimeno, D., & Aulinas, M. (2010). Geomorphological reconstruction and morphometric modelling applied to past volcanism. *International Journal of Earth Sciences*, 99, 645–660. doi: 10.1007/s00531-008-0413-1
- Rodriguez-Gonzalez, A., Fernández Turiel, J. L., Pérez-Torrado, F. J., Hansen Machín, A., Aulinas, M., Carracedo, J. C., ... Paterne, M. (2009). The Holocene volcanic history of Gran Canaria island: Implications for volcanic hazards. *Journal of Quaternary Science*, 24(7), 697–709. doi:10.1002/jqs.1294
- Rodriguez-Gonzalez, A., Fernandez-Turiel, J. L., Perez-Torrado, F. J., Paris, R., Gimeno, D., Carracedo, J. C., & Aulinas, M. (2012). Factors controlling the morphology of monogenetic basaltic volcanoes: The Holocene volcanism of Gran Canaria (Canary Islands, Spain). *Geomorphology*, 136(1), 31–44. doi:10.1016/j.geomorph.2011.08.023
- Ryan, W. B. F., Carbotte, S. M., Coplan, J. O., O’Hara, S., Melkonian, A., Arko, R., ... Zemsky, R. (2009). Global multi-resolution topography synthesis. *Geochemistry, Geophysics, Geosystems*, 10(3), n/a–n/a. doi:10.1029/2008GC002332
- Schmincke, H. U., & Sumita, M. (2010). *Geological evolution of the Canary Islands: A young volcanic archipelago adjacent to the Old African Continent*. Koblenz: Göerres-Druckerei.
- Silver, P. G., Russo, R. M., & Lithgow-Bertelloni, C. (1998). Coupling of South American and African plate motion and plate deformation. *Science*, 279(5347), 60–63. doi:10.1126/science.279.5347.60
- van den Bogaard, P. (2013). The origin of the Canary Island Seamount Province - New ages of old seamounts. *Scientific Reports*, 3(1). <http://www.nature.com/articles/srep02107#supplementary-information> doi:10.1038/srep02107
- Zacsek, K., Troll, V. R., Cachao, M., Ferreira, J., Deegan, F. M., Carracedo, J. C., ... Burchardt, S. (2015). Nannofossils in 2011 El Hierro eruptive products reinstate plume model for Canary Islands. *Scientific Reports*, 5(1). <http://www.nature.com/articles/srep07945#supplementary-information> doi:10.1038/srep07945